Validation of the CQU-DTU-LN1 series of airfoils

W Z Shen[1], W J Zhu[1], A Fischer[1], N R Garcia[1], J T Cheng[1, 2], J Chen[2] and J Madsen[3]

[1]Department of Wind Energy, Technical University of Denmark, DK-2800 Lyngby, Denmark
[2]State Key Laboratory of Mechanical Transmission, Chong Qing University, Chongqing, China
[3]LM Wind Power, Jupitervej 6, 6000 Kolding, Denmark

E-mail: wzsh@dtu.dk

Abstract. The CQU-DTU-LN1 series of airfoils were designed with an objective of high lift and low noise emission. In the design process, the aerodynamic performance is obtained using XFOIL while noise emission is obtained with the BPM model. In this paper we present some validations of the designed CQU-DTU-LN118 airfoil by using wind tunnel measurements in the acoustic wind tunnel located at Virginia Tech and numerical computations with the in-house Q^{3}uic and EllipSys 2D/3D codes. To show the superiority of the new airfoils, comparisons with a NACA64618 airfoil are made. For the aerodynamic features, the designed Cl and Cl/Cd agrees well with the experiment and are in general higher than those of the NACA airfoil. For the acoustic features, the noise emission of the LN118 airfoil is compared with the acoustic measurements and that of the NACA airfoil. Comparisons show that the BPM model can predict correctly the noise changes.

1. Introduction

Design of wind turbine airfoils is a basic but important task for designing wind turbine rotors. Employing an efficient airfoil with a high lift coefficient and a high lift-to-drag ratio can reduce the cost of wind turbine blades, and therefore reduce the cost of energy. On the other hand, noise from wind turbines can give annoyance to the people living nearby which becomes a barrier for further developments of wind energy. Therefore designing highly efficient wind turbines, and at the same time reducing its noise emission are the design goals of future wind turbines.

The design of wind turbine airfoils was started in the 1970's and some pioneering works were carried out on designing wind turbine airfoils such as the Wortmann FX 77-W-series airfoils [1] and the NREL airfoils [2]. Consecutively, Björk [3], Timmer and van Rooij [4], Fuglsang and Bak [5] made some significant contributions in designing the wind turbine airfoils named with their institution's names (FFA, DU and RISØ airfoils).

The design work of the CQU-DTU airfoils [6, 7] was initiated in 2007. It is a product of the research collaboration between Chong Qing University (CQU) in China and Technical University of Denmark (DTU) in Denmark. CQU-DTU-A series of airfoils were designed in 2008. The design objectives of

this series of airfoils are mainly the desirable airfoil aerodynamic characteristics, such as high lift coefficient and lift-to-drag ratio. However, when the size and the power of wind turbines are becoming larger, noise from wind turbines becomes more important. By using the design theory previously developed for designing CQU-DTU-A series airfoils and a modified BPM noise prediction code for airfoil trailing edge (TE) noise [8], the CQU-DTU-LN1 series of airfoils was designed in 2010.

The goal of the present paper is to validate the design of CQU-DTU-LN1 series of airfoils by using both wind tunnel measurements and numerical computations. The experimental validation of the CQU-DTU-LN118 airfoil was carried out in the acoustic wind tunnel at Virginia Tech. Numerical computations are performed by using the modified BPM [8], XFOIL [9], Q^3uic [10] and EllipSys2D/3D [11] [12] codes.

2. Summary of CQU-DTU-LN1 airfoil design

In this section we summarize the design features of the CQU-DTU-LN1 series of airfoils. To represent airfoil shape, Joukowski transformation with combination of trigonometric functions is used. More details about the expression can be found in [6] [7]. The CQU-DTU-LN1 airfoils were designed with an objective function as

$$f(x) = \max(\mu_1 \sum_{i=5}^{10} \lambda_i C_{p1}^i + (1-\mu_1) \sum_{i=5}^{10} \lambda_i C_{p2}^i) \quad (1)$$

where C_{p1}^i and C_{p2}^i are the obtained power coefficients of a blade constructed by using the airfoil with clean and rough airfoil surface at an AOA of i^o, respectively; μ_1 is the weighting factor for a clean airfoil which is determined by the design lifetime and working conditions of a wind turbine. The power coefficient C_p is calculated by using BEM theory under optimum rotor conditions [13].

The design variables are the parameters that can control the airfoil shape. In this paper, the first 6 coefficients in the shape equation are chosen to be the design variables. Geometric compatibility was ensured with the constraints on the location of maximal thickness which is located at a chord position between 20% and 40% measured from the leading edge. The maximal camber-to-chord ratio is located at around 0.04 chords from the leading edge and the location of maximum camber is between 0.5 and 0.53 chords.

In the design stage, the aerodynamic performance was calculated by XFOIL [9]. To estimate the noise generated from an airfoil, a 2D version of the semi-empirical noise model which was developed originally by Brook et al. [14] using acoustic measurements for a NACA 0012 airfoil and the model was shown to give better prediction by using the actual boundary layer quantities at the trailing edge [8].

3. Short description of the experimental setup in the acoustic tunnel at Virginia Tech

To test the aerodynamic and aero-acoustic features of the CQU-DTU-LN118 airfoil, we performed wind tunnel tests in the stability wind tunnel located at Virginia Tech, USA. The acoustic test section and anechoic chambers are shown in Figure 1 where Kevlar windows between the test section and the chambers are used. The 117 microphones in the microphone array are arranged in a 9-armed spiral of 13 microphones with spacing evaluated using a proprietary AVEC array design code. For more information, the reader is referred to [15].

The airfoil model has a chord length of 0.6 m and a span of 1.82 m. It was made from a full aluminum block by RIVAL A/S in Denmark. The airfoil model was equipped with 62 pressure ports (0.5 mm pinhole diameter). To measure the drag, a wake rake pressure technique was used. Inflow turbulence intensity in the aerodynamic test section measured to be less than 0.05%.

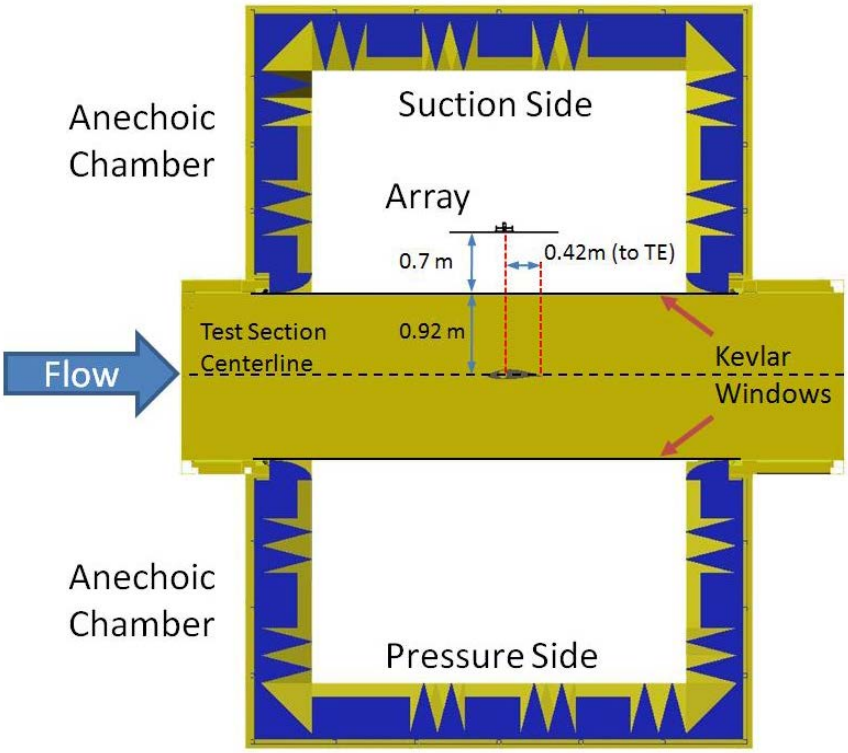

Figure 1. Schematic of test section and 117-channel array position in relation to airfoil.

The acoustic raw data obtained from the microphone measurement were processed with frequency domain beam-forming technique which can extract the sound pressure level of the TE source from the background noise. The time series was measured with a sampling frequency of 51200Hz during a period of 32 seconds and divided into 200 blocks of 8192 samples to compute the averaged cross spectral density matrix. The beam-forming algorithm proposed in [16] was used, which is different to classical beam-forming in two points:

- The diagonal of the cross spectral density matrix is removed
- Refraction affects due to the flow in the wind tunnel test section are accounted for by a ray tracing method.

4. Summary of the employed numerical tools

We select our in-house Q^{3}uic and EllipSys2D codes to compare and validate our airfoil design. The brief description of the two codes is given below.

4.1. Q^{3}uic code

The Q^{3}uic code is a viscous-inviscid interaction technique using strong coupling between the viscous and inviscid parts. The inviscid part is modeled by using a panel method whereas the viscous part is modeled by using the integral form of the laminar and turbulent boundary layer equations with extensions for 3-D rotational effects. The viscous boundary layer equations are solved by using Twaites method for laminar flows and the r and θ integral momentum equations with a set of turbulent closure relations for turbulent flows from Lakshminarayana and Govindan [17] and Drela [9]. Laminar to turbulent transition can be forced at some fixed positions or computed with an e^n transition model. For more details about the solver, the reader is referred to [10]. In the following computations, 140

points distributed with the cosine function are used to discretize the airfoil contour. As an alternative, a Q^3uic version with the Cf closure of Drela [9], noted as Q^3uic1, is also used for comparison.

4.2. EllipSys2D/3D code

The two-dimensional Navier-Stokes solver used here is the EllipSys2D/3D code developed at Technical University of Denmark [11] in collaboration with Risø National Laboratory [12]. The code is based on a finite-volume method with multi-block strategy. This allows it to be run on parallel computers with Message Passing Interface (MPI). The incompressible Navier-Stokes equations are solved by a predictor-corrector method combined with the improved Rhie-Chow interpolation scheme developed in [18]. The pressure Poisson equation is solved by using a 5-level multi-grid technique. Steady RANS computations with k-ω SST turbulence model are carried out on a C-mesh consisting of 448 cells in the tangential direction and 256 cells in the radial direction where the height of the first cell away from the airfoil is in the order of 10^{-5} chords is used.

5. Results

In the experiment of the CQU-DTU-LN118 airfoil made at Virginia Tech, 19 runs were performed at 3 different wind speeds of 30, 45 and 60 m/s which correspond to 3 different Reynolds numbers and 3 different Mach numbers. The first 9 runs were performed with surface pressure taps and far-field microphones whereas the other 10 runs were performed with surface pressure taps and wake rake. To illustrate the high performance of the present airfoil, a NACA64618 airfoil which was tested in the same wind tunnel will be used for comparison.

5.1. Aerodynamic performance

To illustrate the aerodynamic performance of the CQU-DTU-LN1 series of airfoils, we select the case at a tunnel wind speed of 60 m/s which corresponds to a Reynolds number of $2.1\text{x}10^6$. To show the superiority of the airfoil, we compare its performance with a NACA64618 airfoil at Reynolds number of $1.6\text{x}10^6$ for both clean and rough leading edge (LE) cases.

5.1.1. At a Reynolds number of $2.1\text{x}10^6$

The CQU-DTU-LN1 series of airfoils were designed for MW wind turbines. To obtain accurate aerodynamic blade design data under test conditions close to the operating conditions of a blade on the MW turbines, a Reynolds number as high as possible is required. In the experiment performed at Virginia Tech, the highest Reynolds number appearing at the wind speed of 60 m/s is about $2.1\text{x}10^6$. The lift and drag coefficients for a clean CQU-DTU-LN118 airfoil are plotted in Figure 2. From the figure, it is seen that the lift coefficient increases linearly and reaches a maximum lift of 1.77 at an angle of attack of 10.5^o. The drag coefficient is quite small before the airfoil stalls with a minimum Cd of about 0.007. The three numerical methods predict quite well in the linear region up to stall for both Cl and Cd. The XFOIL and EllipSys2D over-predict the maximum lift and the stalled angle of attack whereas the Q^3uic code predicts very well the stall behaviors. The drag coefficient is in general well predicted by all codes. To check if the codes can predict correctly the local forces, surface pressure coefficient is plotted in Figure 3. From the figure, it is seen that the three codes can predict correctly the Cp at the design angles of attack of 6.7^o and 9.6^o.

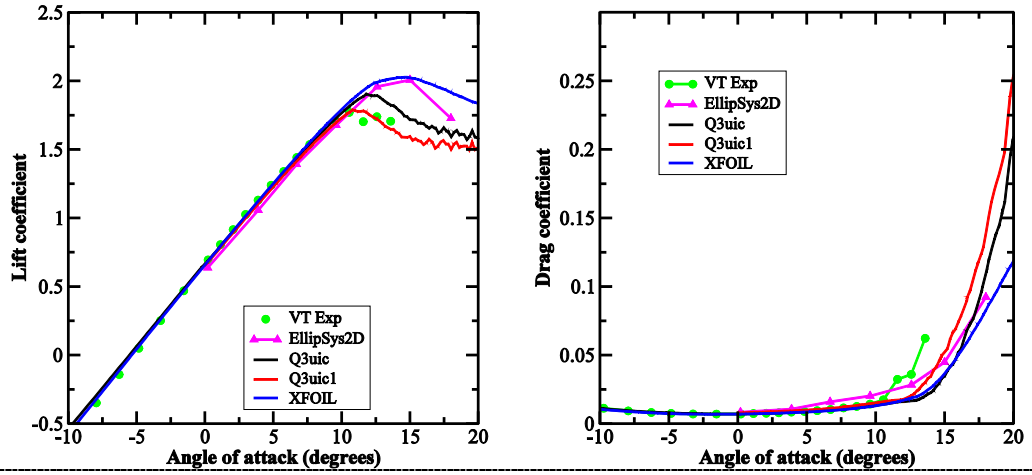

Figure 2. Lift (left) and drag (right) coefficients for flows past a clean CQU-DTU-LN118 airfoil at Re=2.1x10^6.

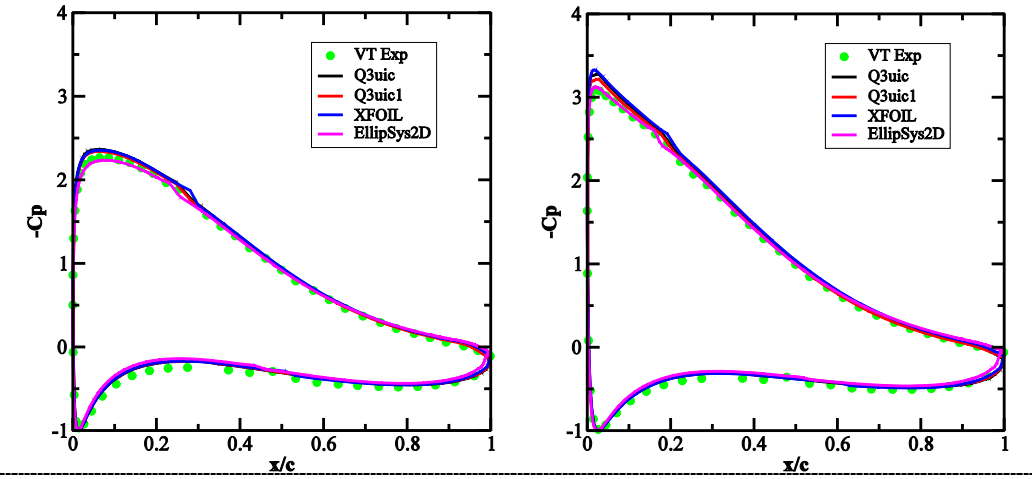

Figure 3. Surface pressure coefficient of flows past a clean CQU-DTU-LN118 airfoil at Re=2.1x10^6 and angles of attack of 6.7^o (left) and 9.6^o (right).

In order to check the sensitivity to LE roughness of the airfoil, standard zigzag trip tapes with a thickness of 0.3 mm (Trip1) and 0.4 mm (Trip2) were placed at 5% chords on the suction side and 10% chords on the pressure side. In Figure 4, the lift and drag coefficients for flows past the tripped CQU-DTU-LN118 airfoil are plotted and results show that their aerodynamic performances are similar. From the figure, it is seen that the airfoil stalls around 8^o with a maximum lift of 1.44 which gives a difference in Cl between a clean and rough airfoil of about 0.33. In general the codes tend to over-predict the maximum lift whereas the Q^{3}uic code with Cf closure of Drela (Q^{3}uic1) almost can predict the maximum lift. For the drag, all codes predict well in the region before stall and under predict in the stall region. This is mainly due to the different treatment of roughness in experiments and computations. It is worth noting that the airfoil was designed with an objective function of Cp in the AOA from 5^o to 10^o which is located in the stall region when tripped. Some improvements could be made if the Q^{3}uic code is used in the airfoil design.

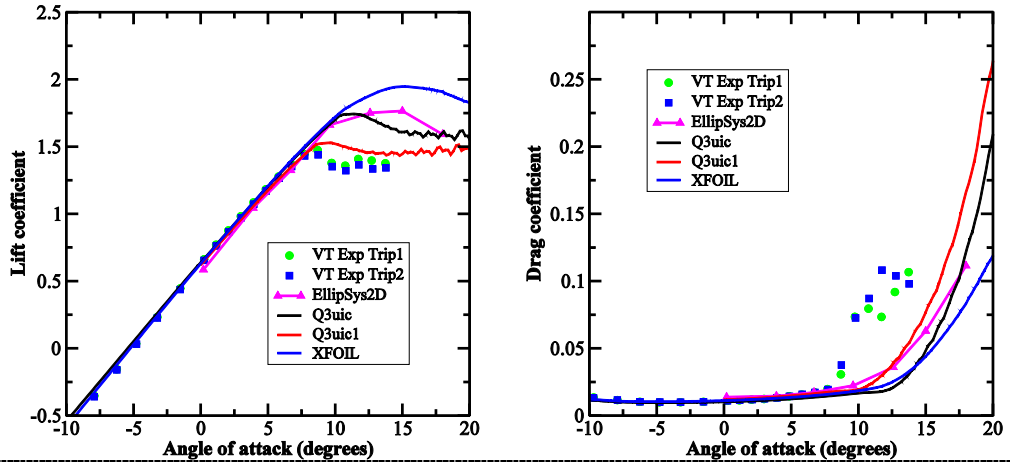

Figure 4. Lift (left) and drag (right) coefficients for flows past a tripped CQU-DTU-LN118 airfoil at Re=2.1x10^6.

In wind turbine design, lift to drag ratio is a very important parameter which can determine the performance of the turbine. The lift to drag ratio of the CQU-DTU-LN118 airfoil is plotted in Figure 5 for both clean and rough cases. In the clean surface case, the experimental Cl/Cd reaches around 148 at an angle of attack of about 6^o. For the numerical codes, both XFOIL and Q^{3}uic can predict correctly the lift to drag ratio while Q^{3}uic1 and EllipSys2D under-predict heavily the ratio due to the too high predictions of drag. In the tripped case, the lift to drag ratio decreases a lot with a maximum of 85 at an angle of attack of 6.7^o. XFOIL can predict correctly the lift to drag ratio while Q^{3}uic over-predicts slightly the ratio, and Q^{3}uic1 and EllipSys2D under-predict slightly it.

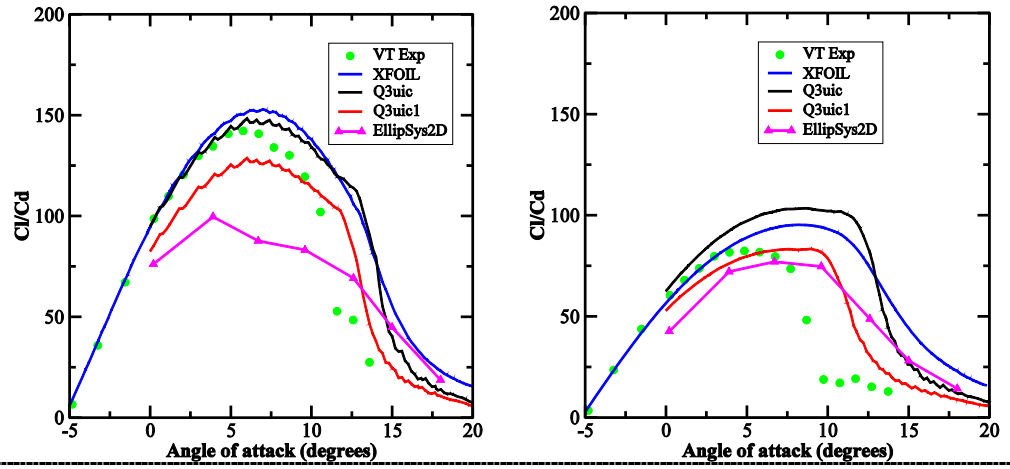

Figure 5. Lift to drag ratio for flows past a clean (left) and tripped with Trip1 (right) CQU-DTU-LN118 airfoil at Re=2.1x10^6.

5.1.2. Comparison with a NACA64618 airfoil

To illustrate the high performance of the CQU-DTU-LN118 airfoil, we choose a NACA64618 airfoil which is used in modern wind turbine blades. Another reason is that this airfoil has been tested in the same wind tunnel. Figure 6 shows lift coefficient for both airfoils with both clean and rough surface at Reynolds number of 1.6x10^6. In the clean case, it is seen that the LN118 airfoil performs better with a

higher design Cl and max Cl while in the rough case the differences between the two airfoils are smaller. It is worth noting that both XFOIL and Q^{3}uic codes predict very well the performance of the NACA airfoil.

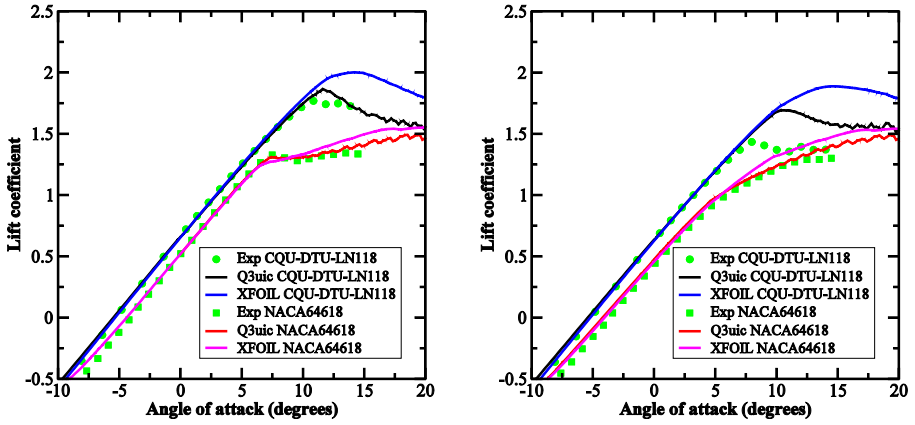

Figure 6. Lift coefficient for flows past a clean (left) and tripped (right) CQU-DTU-LN118 and NACA64618 airfoil at Re=1.6x10^6.

5.2. Acoustic features

The aero-acoustic measurements of the CQU-DTU-LN118 airfoil at Virginia Tech were made by AVEC. Three wind speeds of 30 m/s, 45 m/s and 60 m/s had been considered. To test the noise features of a rough airfoil, the tripped LN118 airfoil was also measured at 45 m/s. To check the design of the CQU-DTU-LN118 airfoil, we compare its noise emission with a NACA64618 airfoil that was tested in the same wind tunnel in 2011. Since the two airfoils are very different with a different zero-lift angle of attack and a different stall angle of attack, it is difficult to compare their noise emission. Since airfoil's Cl and Cl/Cd features are mainly considered when constructing wind turbine blades, we compare here the noise features at a same Cl.

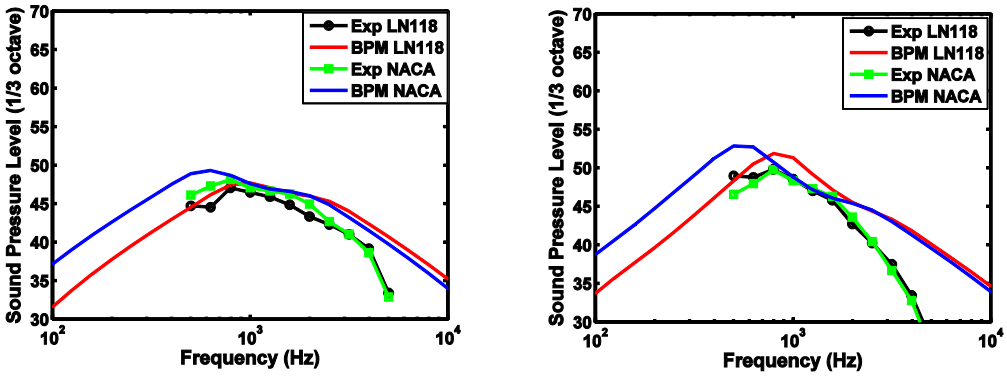

Figure 7. Sound pressure level in 1/3 octave at a distance of 1.62 m and 90^o of noise generated from a CQU-DTU-LN118 and NACA64618 airfoil at a wind speed of 45 m/s and Cl= 0.50 (left) and 0.94 (right).

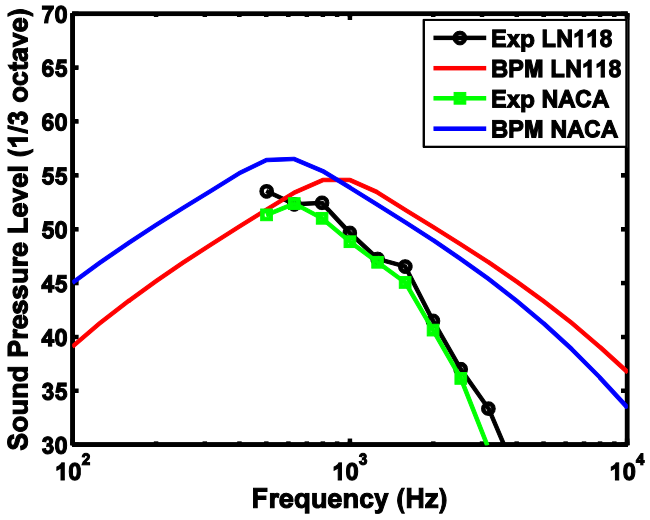

Figure 8. Sound pressure level in 1/3 octave at a distance of 1.62 m and 90^o of noise generated from a CQU-DTU-LN118 airfoil at a wind speed of 45 m/s, an angle of attack of 6^o (Cl= 1.34) and from a NACA64618 airfoil at a wind speed of 45 m/s , an angle of attack of 6.5^o (Cl=1.26).

The sound pressure level calculated at a reference point of 1.62 m and 90^o for flows past the CQU-DTU-LN118 and NACA64618 airfoils at a wind speed of 45 m/s are shown in Figure 7. At the same lift coefficient of 0.50 (Figure 7(left)), the experimental data show that the LN118 airfoil produces a lower noise level in the frequency region below 3000 Hz. Similar results are also seen at Cl=0.94 (Figure 7(right)) Acoustic computations using the BPM model are also plotted in the same figure. From the figure, the BPM model is seen to slightly over-predict noise emission for both airfoils but the prediction of the relative differences between the airfoils can be found from the experimental. The main differences between the two airfoils are seen in the frequency region below 500 Hz. Due to the limitation of the experimental set-up, these features cannot be validated. To show the noise features near the design angle of attack, the sound pressure level for flows past the CQU-DTU-LN118 airfoil at an angle of attack of 6^o and the NACA64618 at an angle of attack of 6.5^o is compared in Figure 8. It is worth noting that the LN118 airfoil at AOA of 6^o has a Cl of 1.34 while the NACA airfoil has a Cl of 1.26. From the figure, it is seen that the BPM model over-predicts slight the noise emission. The total noise emission of the two airfoils calculated with the BPM model is listed in Table 1. From the table, it is seen that the clean CQU-DTU-LN118 airfoil produces less noise of about 2.5 dB than the clean NACA64618 airfoil at a wind speed of 45 m/s and Cl of 0.94.

Table 1. Sound pressure level calculated at an observer position of 1.62 m and 90^o from clean airfoils with a chord of 0.60 m and a span of 1.62 m at a wind speed of 45 m/s.

	Cl=0.50	Cl=0.94
CQU-DTU-LN118	59.58 dB	60.24 dB
NACA 64618	60.61 dB	62.78 dB

When a wind turbine becomes old, its surface is polluted with dust. To consider its noise features, flows past the two airfoils with strip tapes at 5% on the suction side and 10% on the pressure at a wind speed of 45 m/s are considered. The noise emission of the two airfoils is plotted in Figure 9. It is worth noting that the considered Cls in Figure 9 are not exactly the same as in Figure 7 due to the differences

in tunnel correction in the two cases. From the figures, BPM is seen to follow the tendencies of the noise features in general. It is noted that when an airfoil becomes rough, the peak frequency moved to the low frequency region. The total noise emission of the two rough airfoils calculated with the BPM model is listed in Table 2. From the table, it is seen that the rough CQU-DTU-LN118 airfoil produces less noise of about 1.5 dB than the rough NACA64618 airfoil at a wind speed of 45 m/s and Cl of 0.47 and 5 dB at a wind speed of 45 m/s and Cl of 0.90.

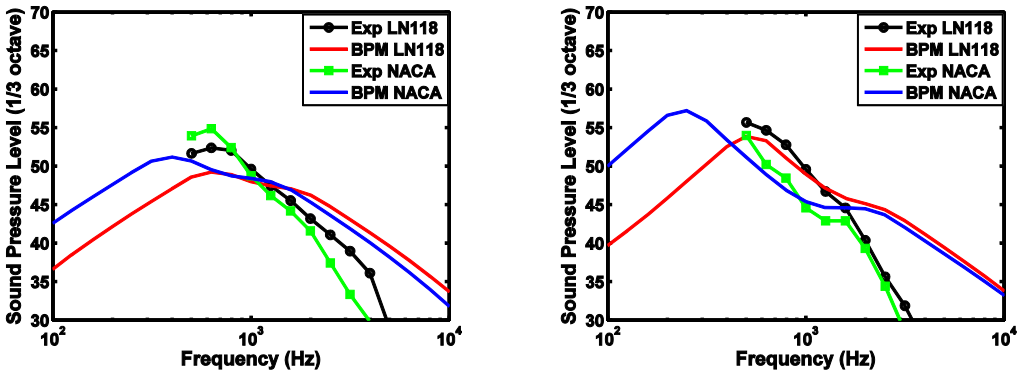

Figure 9. Sound pressure level in 1/3 octave at a distance of 1.62 m and 90^o of noise generated from a tripped CQU-DTU-LN118 and NACA64618 airfoil at a wind speed of 45 m/s and Cl= 0.47 (left) and 0.90 (right).

Table 2. Sound pressure level calculated at an observer position of 1.62 m and 90^o from rough airfoils with a chord of 0.60 m and a span of 1.62 m at a wind speed of 45 m/s.

	Cl=0.47	Cl=0.90
CQU-DTU-LN118	60.93 dB	62.08 dB
NACA 64618	62.48 dB	67.01 dB

6. Conclusions

In this paper validations of the high efficient and low noise CQU-DTU-LN118 airfoil are presented using wind tunnel measurements and numerical computations. The measurements were carried out in the acoustic wind tunnel at Virginia Tech and numerical computations were made with XFOIL, Q^{3}uic, EllipSys2D and BPM codes. For showing the ability of the new airfoil, a NACA64618 airfoil was used for comparison. For the aerodynamic features, the designed Cl and Cl/Cd agrees well with the experiment and are in general higher than those of the NACA airfoil. For the acoustic features, the noise emission of the LN118 airfoil is compared with the acoustic measurements and that of the NACA airfoil. The BPM model predicts a major noise reduction for the LN118 airfoil compared to the NACA64618 in the low frequency range (approx. 100 – 400Hz) when compared at the same lift coefficient. The measurements could not confirm this, because the measurement technique was limited to frequencies above 600Hz. However, the measurements confirmed that the BPM model gives the right tendency of the noise for both airfoils in the measured frequency range. Hence, it is assumed that the predictions by the BPM model also give the right tendency in the low frequency range and that the LN118 airfoil significantly reduces the noise compared to the NACA64618 airfoil. But an experimental validation of the noise emission in the low frequency range has to be performed later to proof our statement.

7. References

[1] Thiele H M 1983 Growian rotor blades: production development, construction and test *NASA TM*-77479
[2] Tangler J L, Somers D M 1987 Status of the special purpose airfoil families *Proc. WINDPOWER'87* San Francisco USA
[3] Björk A 1989 Airfoil design for variable rpm horizontal axis wind turbines *Proc. EWEC'89* Glasgow Scotland
[4] Timmer W A, Van Rooij R 2003 Summary of the Delft university wind turbine dedicated airfoils *Journal of Solar Energy Engineering* **125** 488-496
[5] Fuglsang P, Bak C 2004 Development of the RISØ wind turbine airfoils *Wind Energy* **7** 145-162
[6] Wang X D, Chen J, Shen W Z, Zhang S 2009 Integration study on airfoil profile for wind turbines *China Mechanical Engineering* **20** 211-228
[7] Cheng J T, Chen J, Shen W Z, Zhu W J, Wang X D 2011 Optimization design of airfoil profiles with respect to noise emission of wind turbines *Acta Energiae Solaris Sinica*
[8] Zhu W J, Heilskov N, Shen W Z, Sørensen J N 2005 Modeling of aerodynamically generated noise from wind turbines *Journal of Solar Energy Engineering* **127** 517-528
[9] Drela M 1989 XFOIL: An analysis and design system for low Reynolds number airfoils *Conference on Low Reynolds Number Aerodynamics* University of Notre Dame
[10] Garcia NR, Sørensen JN, Shen WZ 2013 A Strong Viscous-Inviscid Interaction Model for Rotating Airfoils, *Wind Energy*, published online, DOI: 10.1002/we.1669.
[11] Michelsen J A 1992 Basis3D – A platform for development of multiblock PDE solvers. *Technical Report AFM* 1992-05 Technical University of Denmark
[12] Sørensen N N 1995 General purpose flow solver applied over hills *RISØ-R-827(EN)* RISØ National Laboratory Roskilde Denmark
[13] Bak C 2007 Research in aeroelasticity EFP-2006 *RISØ-R-1611(EN)* RISØ National Laboratory Roskilde Denmark
[14] Brooks T F, Pope D S, and Marcolini M A 1989 Airfoil self-noise and prediction *NASA Reference Publication* 1218 National Aeronautics and Space Administration USA
[15] Devenport W J, Burdisso R A, Borgoltz A, Ravetta P and Barone M F 2010 Aerodynamic and acoustic corrections for a Kevlar-walled anechoic wind tunnel *Proc. of the 16th AIAA/CEAS Aeracoustics Conference*
[16] Mueller T J 2002 Aeroacoustic measurements *ISBN* 3-540-41757-5 Springer-Verlag Berlin Heidelberg New York
[17] Lakshminarayana B and Govindan T 1981 Analysis of turbulent boundary layer on cascade and rotor blades of turbomachinery *AIAA journal* **19** 1333-1341
[18] Shen W Z, Michelsen J A and Sørensen J N 2001 Improved Rhie-Chow interpolation for unsteady flow computations *AIAA Journal* **39** 2406-2409

Acknowledgments

This work was supported by the Energy Technology Development and Demonstration Program (EUDP-2011-I, J. nr. 64011-0094) under the Danish Energy Agency. Authors wish to acknowledge the staff at Virginia Tech for performing the wind tunnel tests.